Journal of Thermal Science and Technology

Vol. 7, No. 1, 2012

Molecular Dynamics Study of Condensation/Evaporation and Velocity Distribution of N-Dodecane at Liquid-Vapour Phase Equilibria*

Jian-Fei XIE**, Sergei S SAZHIN** and Bing-Yang CAO***

** Sir Harry Ricardo Laboratories, School of Computing, Engineering and Mathematics, University of Brighton, Cockcroft Building, Brighton BN2 4GJ, UK

E-mail: s.sazhin@brighton.ac.uk

*** Department of Engineering Mechanics, Tsinghua University, Beijing 100084, China

Abstract

Some recent results of molecular dynamics simulations of the condensation/evaporation and velocity distribution of n-dodecane ($C_{12}H_{26}$), the closest approximation to Diesel fuel, at a liquid-vapour interface in equilibrium state are briefly described. It is shown that molecules at the liquid surface need to gain relatively large translational energy to evaporate. Vapour molecules with large translational energy can easily penetrate deep into the transition layer and condense in the liquid phase. The evaporation/condensation coefficient is shown to be controlled mainly by the translational energy. The properties of the velocity distribution functions of molecules at the liquid, interface and vapour regions are summarised. It has been shown that the distribution functions of evaporated and reflected molecules for the velocity component normal to the surface deviate considerably from the Maxwellian, while the distribution function for all molecules leaving this surface (evaporated and reflected) is close to Maxwellian. The evaporation coefficient has been shown to increase with increasing molecular energy in the direction perpendicular to the surface. These properties have been recommended to be taken into account when formulating boundary conditions for kinetic modelling.

Key words: Molecular Dynamics Simulations, Condensation/Evaporation, Velocity Distribution Function, N-Dodecane

1. Introduction

A widely used engineering approach to the modelling of evaporation/condensation processes is based on the hydrodynamic approximation. The limitation of this approach, even in the case of evaporation at high pressures, has been discussed in a number of papers [1-5]. In these papers the evaporation of n-dodecane (the nearest approximation for Diesel fuel) has been considered and a new model for the analysis of droplet heating and evaporation has been developed on the basis of the combination of kinetic and hydrodynamic approaches. In the immediate vicinity of droplet surfaces (up to about one hundred molecular mean free paths), the vapour and ambient gas dynamics have been studied by solving the Boltzmann equation (kinetic region), while at larger distances it has been based on the hydrodynamic equations (hydrodynamic region) (see Fig. 1). Mass, momentum and energy fluxes have been conserved at the interface between these regions.

*Received 6 Jan., 2012 (No. 12-0007)
[DOI: 10.1299/jtst.7.288]

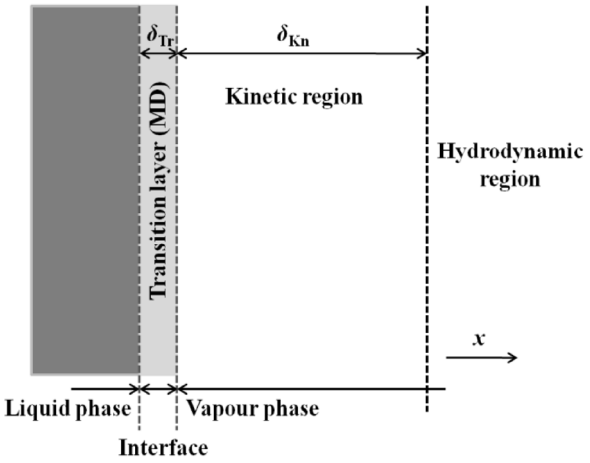

Figure 1: A schematic presentation of different regions related to hydrodynamic and kinetic modelling, and molecular dynamics simulations. δ_{Tr} and δ_{Kn} are the thicknesses of the transition layer and kinetic region, respectively.

The predictions of this model have been shown to be as accurate as those of the model based on the kinetic equations in the whole domain, but both differed considerably (up to 10%) from the predictions of the hydrodynamic models for Diesel engine-like conditions. The practical applications of this combined or kinetic modelling, however, require the specification of some special boundary conditions at the droplet surface and at the interface between the kinetic and liquid regions (see Fig. 1). The kinetic boundary condition at the interface between vapour and its condensed phase has been presented as [6]:

$$f^{out} = \sigma_e f^e + (1 - \sigma_e) f^r \quad (v_x > 0), \tag{1}$$

where f^{out} is the overall distribution function of molecules leaving the interface from the liquid phase, σ_e is the evaporation coefficient, f^e is the distribution function of evaporated molecules, f^r is the distribution function of reflected molecules and v_x is the velocity component normal to the interface. In the equilibrium state the evaporation and condensation coefficients are equal. They will be referred to as the evaporation/condensation coefficient. In the above mentioned papers [1-5], it has been implicitly or explicitly assumed that the distribution function f^e is isotropic Maxwellian with the temperature equal to the liquid surface temperature. The values of the evaporation/condensation coefficients have been assumed equal to 0.04 and 0.5 (the minimal and average value of this parameter for water) [1] or 1 [2-5]. None of these assumptions have been rigorously justified. The only practical way to perform this justification would be to base it on the molecular dynamic simulation at the interface region (transition layer, see Fig. 1).

Most of the previous studies have applied the molecular dynamic approach to the analysis of the evaporation and condensation processes, involving monatomic or relatively simple polyatomic molecules, such as argon, water or methanol [7-11]. In our previous studies [12, 13], molecular dynamics simulations have been performed to study the evaporation and condensation of n-dodecane ($C_{12}H_{26}$) at liquid-vapour phase equilibrium using the modified OPLS (Optimized Potential for Liquid Simulation) model. The properties at the interface were studied and the evaporation/condensation coefficient was estimated. Typical molecular behaviours in the evaporation and condensation processes were presented and discussed.

The aim of this paper is to summarise the main findings of [12, 13] and present some new results of the analysis of the evaporation and condensation processes at the

liquid-vapour interface, obtained after the publications of [12, 13]. Section 2 presents the molecular dynamic simulations of n-dodecane ($C_{12}H_{26}$) in liquid-vapour equilibrium. The results of the analysis are presented and discussed in Section 3. The conclusions are drawn in Section 4.

2. Molecular dynamics simulation

2.1 Interatomic potentials

The interactions in chain-like molecular structures are modelled using the Optimized Potential for Liquid Simulation (OPLS) [12, 13] and the united atom model, including the methyl (CH_3) and methylene (CH_2) groups [14], schematically illustrated in Fig. 2 for n-dodecane.

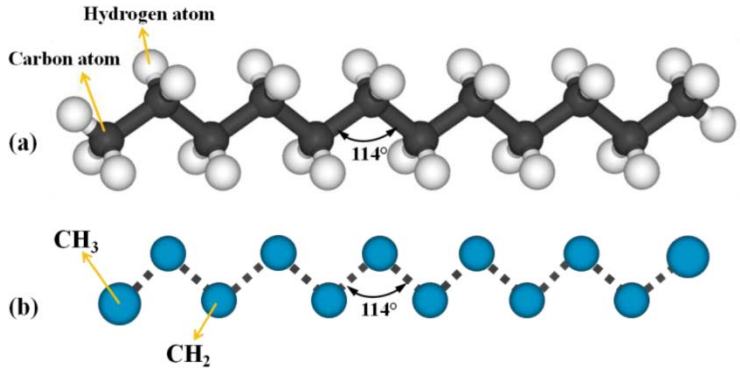

Figure 2: Molecular structure of n-dodecane ($C_{12}H_{26}$) (a) and the corresponding united atom model (b).

As in [12, 13], the non-bonded interactions between atoms are described by the truncated Lennard-Jones (L-J) 12-6 potential [15]:

$$u^{LJ}(r_{ij}) = 4\varepsilon_{ij}\left[\left(\frac{\sigma_{ij}}{r_{ij}}\right)^{12} - \left(\frac{\sigma_{ij}}{r_{ij}}\right)^{6}\right]. \quad (2)$$

The energy parameters of CH_2 and CH_3 groups (atoms) are ε_{CH_2}/k_B =47 K and ε_{CH_3}/k_B =114 K respectively, and the energy parameter between CH_2 and CH_3 groups is estimated as $\varepsilon_{CH_2-CH_3}/k_B = \sqrt{\varepsilon_{CH_2}\varepsilon_{CH_3}}/k_B$ =73.2 K (k_B is the Boltzmann constant). The diameters of the methylene and methyl groups are assumed to be equal and estimated as $\sigma =$ 3.93×10^{-10} m. The L-J 12-6 interaction is truncated at 13.8×10^{-10} m.

The interactions within the chains include bond bending and torsion with the bond length constrained at 1.53×10^{-10} m. The bond bending potential between the three atoms is estimated as [16]:

$$u^{bend}(\theta) = \frac{1}{2}k_\theta(\theta - \theta_0)^2, \quad (3)$$

where the bending coefficient is estimated as k_θ/k_B =62,500 K/rad^2, and the equilibrium angle is θ_0 =114° (see Fig. 2). The torsion potential between four atoms is estimated as [17]:

$$u^{tors}(\emptyset) = c_0 + 0.5c_1(1 + cos\emptyset) + 0.5c_2(1 - cos2\emptyset) + 0.5c_3(1 + cos3\emptyset), \quad (4)$$

where c_0/k_B =0 K, c_1/k_B =355 K, c_2/k_B =-68.19 K, c_3/k_B =791.3 K and $\emptyset$ is the dihedral angle (equal to 180° for the equilibrium state).

2.2 Input parameters

As in [13], a system of 720 n-dodecane ($C_{12}H_{26}$) molecules (8640 CH_3 and CH_2 groups) is considered in a three-dimensional rectangular simulation box of $L_x \times L_y \times L_z = 64.24\sigma \times 16.48\sigma \times 16.48\sigma$, where σ is the reduced length, the value of which is given in Table 1, for liquid temperatures 400 K, 450 K, 500 K and 550 K. This size of box corresponds to 25.25 nm×6.48 nm×6.48 nm. These molecules have initially been oriented along the x axis and placed in the middle of the simulation box (see Fig. 3(a)). They have zigzag configurations (see Fig. 2), and the number of molecules chosen is 5 in the x direction and 12 in both y and z directions.

The equations of motion of the atoms have been integrated using the Verlet leapfrog method [15]. The bond lengths are constrained by the SHAKE scheme [15]. The time step in all simulations has been taken equal to $0.002\,\tau$, which corresponds to 5 fs. Periodic boundary conditions have been applied in all directions. Reduced units have been used for most physical parameters as indicated by the superscript "*" in Table 1.

Table 1: Reduced parameters used in the MD simulations (reproduced from [13]).

Parameters	Values
Mass (m^*)	m_{CH_2} =2.3252×10^{-26} kg
Energy (ε^*)	ε_{CH_2} =0.6486×10^{-21} J
Length (l^*)	σ =3.93×10^{-10} m
Temperature (T^*)	ε_{CH_2}/k_B =47 K
Density (ρ^*)	m_{CH_2}/σ^3 =382.961 kg/m^3
Time (t^*)	$\tau = \sigma\sqrt{(m/\varepsilon_{CH_2})}$=2.353×10^{-12} s
Velocity (v^*)	σ/τ =167 m/s

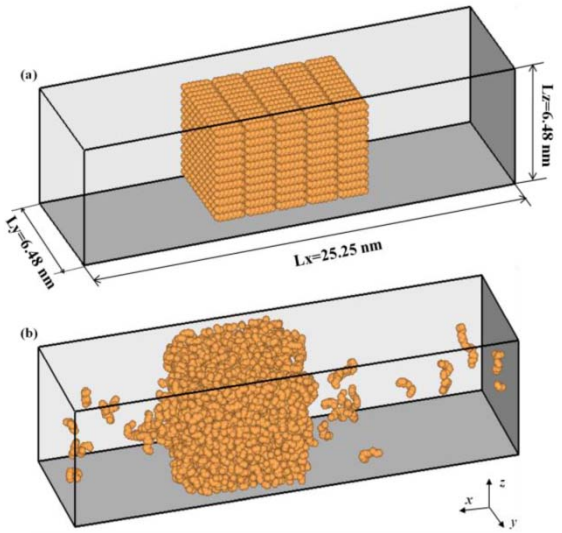

Figure 3: Snapshots of the simulation box: initial state (a) and liquid-vapour equilibrium state at 500 K (b).

The system has been relaxed with a constraint of fixed homogeneous and isotropic temperature. The molecules started to relocate within the liquid phase and to evaporate gradually. Typically the system requires 15,000 ps to reach an equilibrium state. Finally the liquid film was sandwiched between the layers of the vapour phases (see Fig. 3(b) for temperature 500 K; similar results were obtained for temperatures 400 K, 450 K and 550 K [13]). Then we began to sample data for another 5,000 ps. The positions of the two liquid-vapour interfaces were identified by the density profiles. The interface parameters,

such as density and evaporation/condensation coefficient, were obtained by averaging them over these 5,000 ps.

3. Simulation results and discussion

3.1 Interfacial properties

After time-averaged over 5,000 ps during a steady state period, density profiles and the liquid-vapour coexistence at liquid temperatures 400 K, 450 K, 500 K and 550 K were obtained [13]. These profiles agreed with the results of Monte Carlo simulations [14] and the experimental data [18]. As follows from these profiles, at higher liquid temperatures, the densities of the liquid phase are lower as expected. The critical temperature and density were estimated to be about 720 K and 45 kg/m^3.

The thickness of the transition layer at the liquid-vapour interface (interface thickness) was defined as the thickness of the region where the bulk vapour phase changes to the bulk liquid phase. According to this definition, the interface thickness of n-dodecane is estimated to be about 2.3-3.5 nm [13]. This is noticeably larger than that of argon [9], water [9] and methanol [11]. For chain-like n-dodecane ($C_{12}H_{26}$) molecules, the large thickness of the transition layer would be a barrier for vapour molecules to be condensed or for molecules leaving the liquid to be evaporated. Hence, the larger thickness of the transition layer at high temperatures would result in smaller evaporation/condensation coefficients. This is discussed in Section 3.3.

3.2 Evaporation and condensation behaviours

The mechanism of evaporation and condensation of n-dodecane ($C_{12}H_{26}$) has been studied in detail by recording the trajectories and translational energies (normalized by ε_{CH_2} given in Table 1) of molecules at T_l=500 K, and some examples are shown in Figs. 6-9 of [13]. Some further examples are shown in Figs. 4-7. As follows from Fig. 4, the molecule escapes from the bulk liquid and is evaporated (see Fig. 4(a)) when its translational energy abruptly increases (see Fig. 4(b)). Fig. 5 shows how the condensation of the molecule is accompanied by the reduction of its translational energy. This energy in the liquid phase remains close to the mean kinetic energy in the system. The evaporation and condensation behaviours shown in Figs. 4 and 5 allow us to conclude that the translational energy plays an important role in the evaporation and condensation processes. The effect of the translational energy on the evaporation and condensation processes of n-dodecane ($C_{12}H_{26}$) is similar to that for monatomic molecules of argon [7] and polyatomic molecules of water and methanol [8]. This supports the idea of activation energy in the liquid-vapour transition, which follows from the transition state theory [8]. The transition layer leads to building of a three dimensional structure at the liquid-vapour interface with a kind of interfacial resistance as discussed in Section 3.1. The fact that the molecules in the transition layer preferentially lie parallel to the interface is expected to contribute to blocking of the molecular evaporation and condensation [12]. In Figs. 6 and 7, examples of reflection condensation and evaporation are shown. In the case shown in Fig. 6, the activated molecule from the liquid phase collides with other molecules at the interface and returns to its original liquid phase. The time evolution of the energy of the molecule during this period is quite stable because no phase transition takes place. We can see, however, a small increase in energy when the molecule enters the interface region. In the case shown in Fig. 7, the energy of the molecules increases when it approaches the interface, and then decreases deep in the vapour phase.

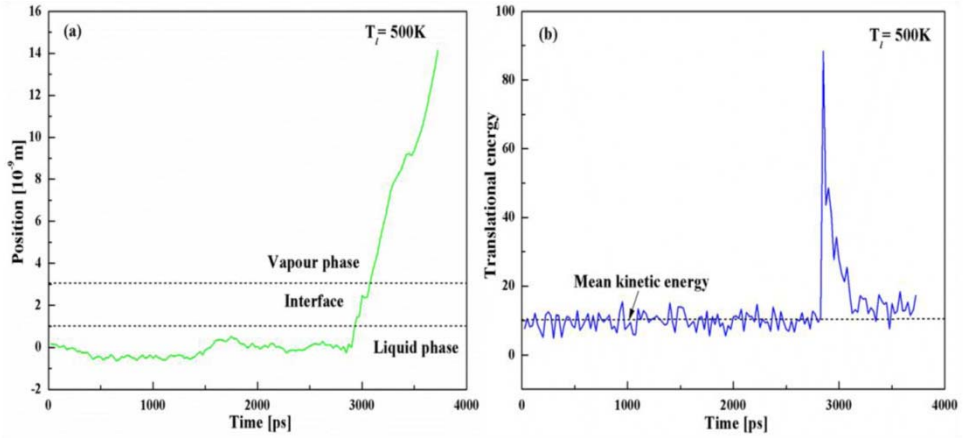

Figure 4: A typical time history of an evaporating molecule: (a) trajectory of the molecule; (b) variations in its translational energy.

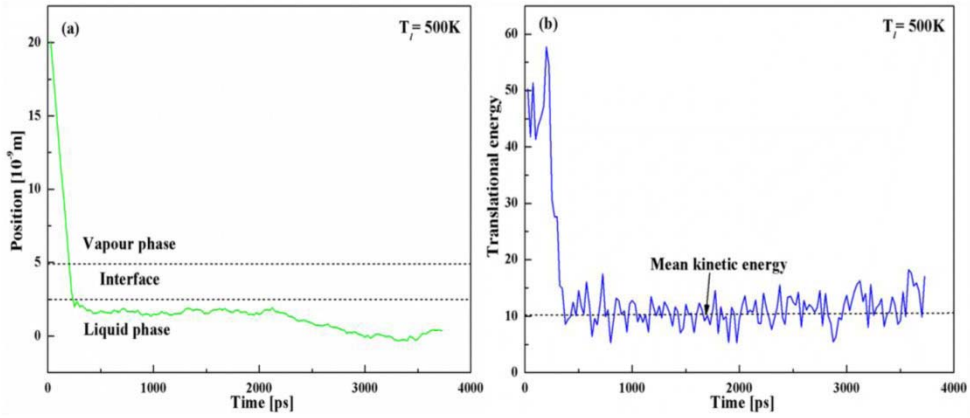

Figure 5: A typical time history of a condensing molecule: (a) trajectory of the molecule; (b) variations in its translational energy.

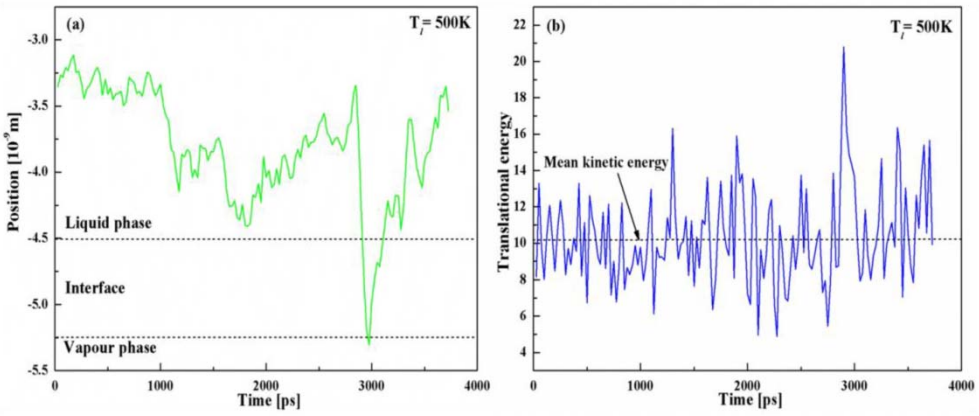

Figure 6: A typical time history of a reflection condensation molecule: (a) trajectory of the molecule; (b) variations in its translational energy.

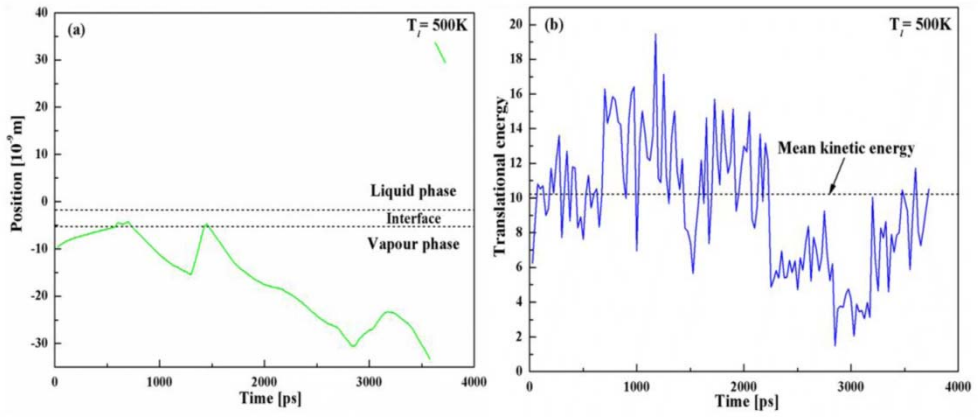

Figure 7: A typical time history of a reflection evaporation molecule: (a) trajectory of the molecule; (b) variations in its translational energy.

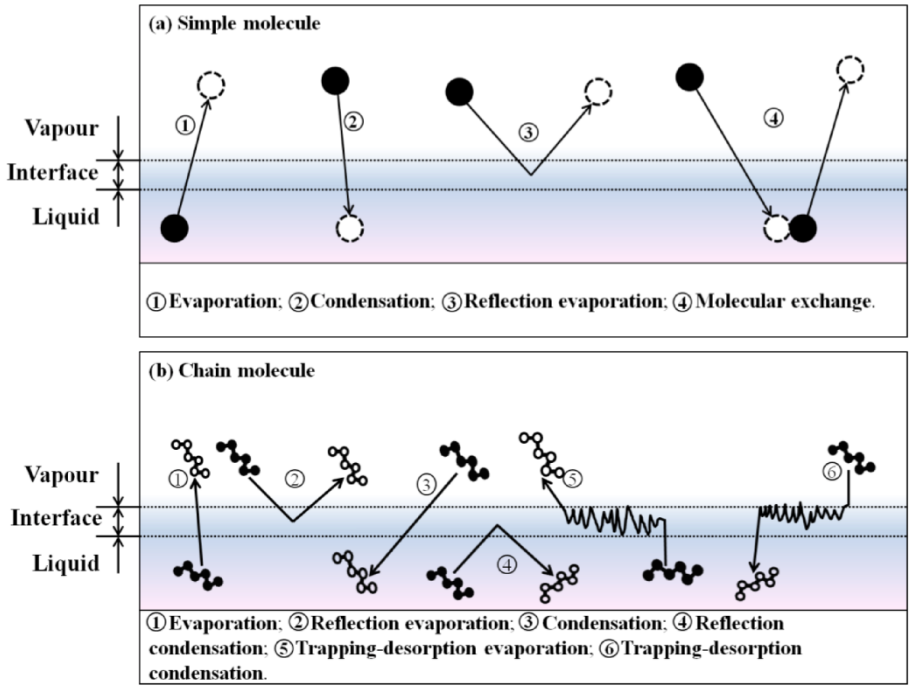

Figure 8: Typical evaporation and condensation behaviours of simple molecules (a) and n-dodecane chains (b). Reprinted with permission from Figure 9 of the paper by Cao, B.-Y., Xie, J.-F., Sazhin, S. (2011), Molecular dynamics study on evaporation and condensation of n-dodecane at liquid-vapour phase equilibria, Journal of Chemical Physics, **134**, 164309. Copyright 2011, American Institute of Physics.

Apart from relatively simple cases shown in Figs. 4-7, a number of other evaporation and condensation scenarios have been considered in the literature as discussed in [12]. Several evaporation and condensation behaviours of simple molecules, such as argon, methanol and water, are summarised in Fig. 8(a). As follows from our analysis, the behaviour of chain molecules can be more complex as shown in Fig. 8(b). The evaporation and condensation behaviours of simple molecules normally include spontaneous evaporation/condensation (typically abbreviated as evaporation/condensation), reflection evaporation, and molecular exchange. The behaviours of chains include spontaneous evaporation/condensation, reflection evaporation/condensation, and trapping-desorption

evaporation/condensation. Spontaneous evaporation/condensation and reflective evaporation are the same for simple and chain molecules. We have not, however, observed any cases of molecular exchange for chain molecules. This may be because, in contrast to simple molecules, chain molecules collide with several molecules in the liquid simultaneously, and the energy transferred to individual molecules appears to be insufficient to remove new molecules from the liquid. To the best of our knowledge, reflection condensation has never been reported for simple molecules. This may be because the collision cross-sections of chain molecules in the interface region are larger, compared with simple molecules. Hence the likelihood of chain molecules which leave the bulk liquid and return to its condensed phase from the vapour-liquid interface is higher, compared with simple molecules. Note that even for chain molecules, this case is rarely observed. Also, trapping-desorption evaporation/condensation has never been reported for simple molecules. In this case, the chains can be trapped inside the liquid-vapour interface for a long time, and lose memory of their origin: vapour or liquid.

3.3 Evaporation/condensation coefficient

The evaporation coefficient σ_e is defined as the ratio of the actual mass flux of the evaporated molecules j_e to its maximum value $j_m = \rho_v\sqrt{k_B T_l/(2\pi m)}$, and ρ_v is the density of saturated vapour. The condensation coefficient σ_c is defined as the ratio of the actual mass flux of condensed molecules j_c to j_m. Under an equilibrium condition, the condensed mass flux should be equal to the evaporated mass flux, *i.e.* $j_c = j_e$. Hence, we have $\sigma_c = \sigma_e$.

We have calculated the condensed mass flux j_c and the evaporated mass flux j_e by counting the number of molecules crossing a unit area per unit time at the interface zone. The following results refer to the condensation coefficient, which does not undermine the generality of our analysis. Based on the transition state theory [8], the condensation coefficient is given by the following expression:

$$\sigma_c = \left[1 - \left(\frac{V^l}{V^g}\right)^{1/3}\right] \exp\left[-\frac{1}{2}\frac{1}{\left(\frac{V^g}{V^l}\right)^{1/3} - 1}\right], \tag{5}$$

where V^l and V^g are specific volumes of the liquid and gas.

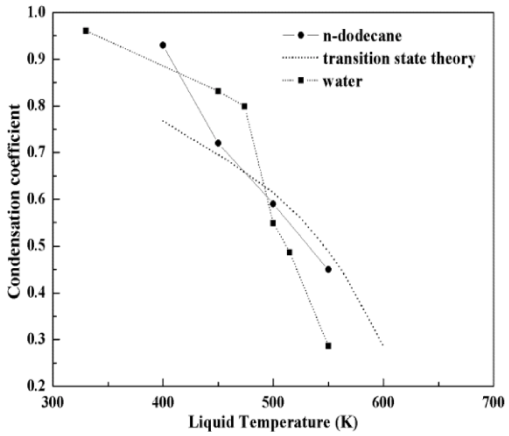

Figure 9: The condensation coefficient versus liquid temperature obtained for n-dodecane using the MD simulations (filled circles) and predicted by Eq. (5) (dashed curve), and reported in [8] for water (filled squares).

The condensation coefficient of n-dodecane has been calculated for liquid temperatures T_l = 400 K, 450 K, 500 K and 550 K [13]. The plots of σ_c versus the liquid temperatures

for n-dodecane are shown in Fig. 9. The results which follow from Eq. (5) and those reported for water are also given in Fig. 9. The plots in this figure are reproduced from the more general Fig. 10 of [13].

As follows from Fig. 9, the condensation coefficient for n-dodecane decreases from about 0.93 at 400 K to about 0.45 at 550 K. The values of the condensation coefficient predicted by the transition state theory using Eq. (5) have been obtained using the densities of the liquid and vapour phases in the MD simulations. The MD data for the condensation coefficient of water [8] (filled squares) illustrate behaviour similar to that of n-dodecane.

The condensation coefficient for complex polyatomic molecules was expected to be lower than that for simpler molecules due to constraints imposed by the rotational motion of molecules in the liquid phase [19]. However, in our MD simulations, it has been found that the rotational energy has no noticeable effect on this coefficient and its value is mainly controlled by the translational energy which is in agreement with the previously reported results [9, 12]. On the other hand, based on the transition state theory, we can expect that this coefficient is close to unity at low temperatures when $(V^g/V^l)^{1/3}$ is large, and decreases with increasing temperature due to the decrease of the ratio $(V^g/V^l)^{1/3}$. This trend is consistent with the prediction of our MD simulations.

3.4 Velocity distribution function

As mentioned in Section 1, it is generally assumed that the distribution functions of the evaporated molecules and the molecules entering the kinetic region from the hydrodynamic one are isotropic Maxwellian. In our previous study [12, 13], however, we found that the distribution function of evaporating molecules may deviate from the isotropic Maxwellian one. The normalized distribution function of translational velocities of the mass centres of molecules can be calculated as [11]:

$$F_j = \frac{1}{\rho N_s \Xi_p \Xi_v^j} \sum_{N_s} \sum_{i \in \left(\Xi_p \cap \Xi_v^j\right)} m_i, \tag{6}$$

where F_j is the distribution of the j component of the translational velocity ($F_j = F_{x,y,z}$), Ξ_p is a volume element in the physical space, Ξ_v^j is a one-dimensional volume element of the j direction in the three-dimensional molecular velocity space, $\Xi_p \cap \Xi_v^j$ denotes a four-dimensional volume element in the six-dimensional physical/velocity phase, and m_i are masses of individual molecules assumed to be the same. The relation between f_j and F_j is $f_j = \rho F_j$. Σ_{Ns} indicates the summation over N_s =10,000 samples.

The velocity distribution function was found by sampling the velocities of the molecules in control volumes of thickness $0.642\sigma = L_x/100$ in three regions: inside the liquid phase, interface and vapour phase. It was shown that the distributions of molecules for y- and z-velocity components v_y and v_z tangential to the interface at the liquid temperatures 500 K and 550 K are close to isotropic Maxwellian [13]. This distribution of the x-velocity component v_x normal to the interface for the same temperatures 500 K and 550 K in the liquid phase and in the interface was also shown to be close to isotropic Maxwellian. This distribution in the vapour phase, however, tended to the Maxwellian but with higher temperature in the direction perpendicular to the interface (x-direction) than in the directions parallel to the interface (y and z directions). This means that the evaporated molecules have larger average translational energies in the direction perpendicular to the interface than the corresponding energies in the direction parallel to the interface. The same phenomenon has also been observed in the MD simulations of argon [7].

Although we appreciate that this result needs to be confirmed by MD simulations with much larger numbers of molecules, we believe that the traditional approach to the

formulation of the boundary conditions in kinetic modelling, when the distribution function of the evaporated molecules is assumed to be isotropic Maxwellian with the same temperatures for all velocity components, needs to be revised.

The normalized distribution function of molecules leaving the droplet surface in the direction perpendicular to this surface(F_x^M) is linked with the normalized distribution functions of evaporated (F_x^e) and reflected (F_x^r) molecules by the following equation

$$\rho^+ F_x^M = \rho^e F_x^e + \rho^r F_x^r,$$

where $\rho^+ = \rho^e + \rho^r$ is the total density of molecules leaving the droplet surface, ρ^e is the density of evaporated molecules, and ρ^r is the density of reflected molecules. The plots of F_x^M, F_x^e and F_x^r versus v_x, as inferred from our MD calculations, are shown in Fig. 10.

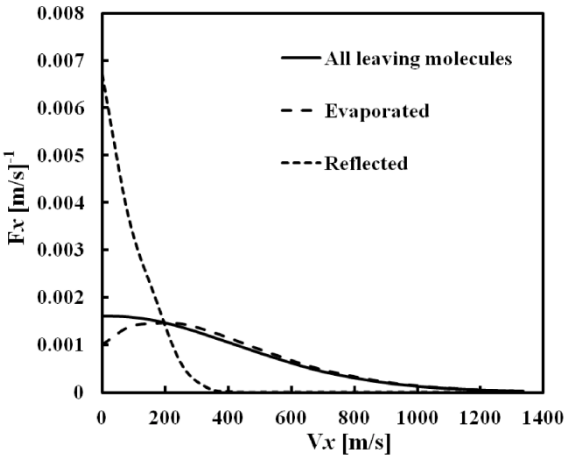

Figure 10: Normalized velocity distributions of evaporated and reflected molecules from the vapour-liquid interface and that of all molecules leaving this surface at T_l=500 K.

As can be seen from Fig. 10, for the velocity component normal to the interface v_x, the distribution function for all molecules leaving the surface is close to isotropic Maxwellian, but these distributions for evaporated and reflected molecules noticeably deviate from the Maxwellian. The distribution function of evaporated molecules is less than Maxwellian at small velocities but greater than Maxwellian at high velocities. The distribution function of reflected molecules, however, is greater than Maxwellian at small velocities but less than Maxwellian at high velocities. Thus, the main contribution to the molecules leaving the droplet surface at small velocities comes from the reflected molecules, while the main contribution to these molecules leaving the droplet surface at high velocities comes from the evaporated molecules.

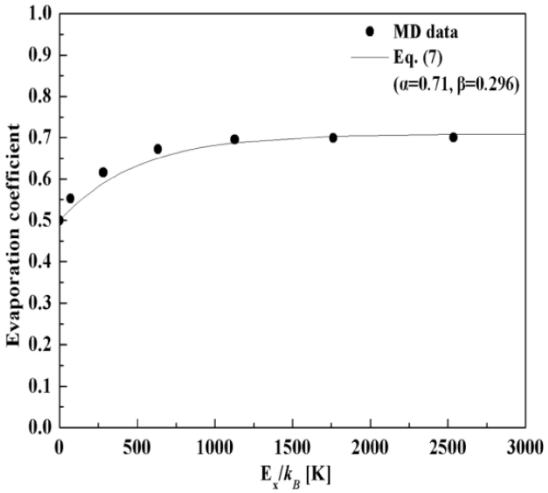

Figure 11: Evaporation coefficient as a function of translational energy E_x/k_B at T_l=500 K.

Also, the ratios of the evaporated molecules to all molecules leaving the interface (evaporation coefficient) have been investigated at various velocities. The results are shown in Fig. 11 by filled circles. Following [7], these results are approximated by the formula

$$\sigma_e = \alpha\left[1 - \beta exp\left(-\frac{E_x}{k_B T_l}\right)\right], \tag{7}$$

where $E_x = \frac{1}{2}mv_x^2$ is the translational energy of molecules in the direction normal to the interface, and α and β are fitting constants which are determined by the liquid temperature; they are estimated as α=0.71, β=0.296. Assuming that the distribution function of the molecules leaving the interface is Maxwellian

$$F_x^M = \left(\frac{m}{2\pi k_B T_l}\right)^{1/2} exp\left(-\frac{E_x}{k_B T_l}\right), \tag{8}$$

we can estimate the average value of the evaporation coefficient as

$$\bar{\sigma}_e = \frac{1}{(k_B T_l/2\pi m)^{1/2}} \int_0^\infty \sigma_e F_x^M dv_x = \alpha\left(1 - \frac{\beta}{2}\right). \tag{9}$$

The normalized velocity distribution functions of evaporated and reflected molecules (F_x^e and F_x^r) can be obtained from the following relation [7]

$$F_x^e = \frac{\sigma_e}{\bar{\sigma}_e} F_x^M = \frac{1-\beta exp(-E_x/2k_B T_l)}{1-\beta/2}\left(\frac{m}{2\pi k_B T_l}\right)^{1/2} exp\left(-\frac{E_x}{k_B T_l}\right), \tag{10}$$

$$F_x^r = \frac{1-\sigma_e}{1-\bar{\sigma}_e} F_x^M = \frac{1-\alpha+\alpha\beta exp(-E_x/2k_B T_l)}{1-\alpha+\alpha\beta/2}\left(\frac{m}{2\pi k_B T_l}\right)^{1/2} exp\left(-\frac{E_x}{k_B T_l}\right). \tag{11}$$

4. Conclusions

The evaporation and condensation of n-dodecane ($C_{12}H_{26}$), the closest approximation to Diesel fuel, have been investigated using the molecular dynamics (MD) simulation technique. Some results of this investigation are presented. It has been pointed out that the molecules at the liquid surface need to gain relatively large translational energy to evaporate. Vapour molecules with high translational energy can easily penetrate deep into the transition layer and condense in the liquid phase. The values of the evaporation/condensation coefficient at various liquid phase temperatures have been estimated and are shown to be in agreement with the predictions of the transition state theory. The properties of molecular velocity distribution functions in the liquid phase, the interface and vapour phases have been summarised. It has been shown that the distribution

functions of evaporated and reflected molecules for the velocity component normal to the surface deviate considerably from the Maxwellian, while the distribution function for all molecules leaving this surface is close to Maxwellian. The evaporation coefficient has been shown to increase with increasing molecular energy in the direction perpendicular to the surface. The normalized distribution functions of evaporated and reflected molecules have been estimated. It is recommended that the results are taken into account when formulating boundary conditions in kinetic modelling.

Acknowledgements

The authors are grateful to EPSRC (grant EP/H001603/1) of the UK, the National Natural Science Foundation of China (grant 50976052), and the Cross-discipline Foundation of the Tsinghua National Laboratory for Information Science and Technology (TNList) for the financial support of this project.

References

[1] A.P. Kryukov, V.Y. Levashov, and S.S. Sazhin, "Evaporation of diesel fuel droplets: kinetic versus hydrodynamic models," Int. J. Heat Mass Transfer 47: 2541-2549 (2004).

[2] S.S. Sazhin, I.N. Shishkova, A.P. Kryukov, V.Yu. Levashov, and M.R. Heikal, "Evaporation of droplets into a background gas: kinetic modelling," Int. J. Heat Mass Transfer 50: 2675-2691 (2007).

[3] S.S. Sazhin and I.N. Shishkova, "A kinetic algorithm for modelling the droplet evaporation process in the presence of heat flux and background gas," Atomization Sprays 19: 473-489 (2009).

[4] S.S. Sazhin, I.N. Shishkova, and M.R. Heikal, "Kinetic modelling of fuel droplet heating and evaporation: calculations and approximations," Int. J. of Engineering System Modelling and Simulation 2: 169-176 (2010).

[5] I.N. Shishkova and S.S. Sazhin, "A numerical algorithm of kinetic modelling of evaporation processes," J. Comput. Phys. 218: 635-653 (2006).

[6] C. Cercignani, *The Boltzmann Equation and its Application* (Springer-Verlag, Berlin, 1988).

[7] T. Tsuruta, H. Tanaka, and T. Masuoka, "Condensation/evaporation coefficient and velocity distributions at liquid-vapour interface," Int. J. Mass Heat Transfer 42: 4107-4116 (1999).

[8] G. Nagayama and T. Tsuruta, "A general expression for the condensation coefficient based on transition state theory and molecular dynamics simulation," J. Chem. Phys. 118: 1392-1399 (2003).

[9] T. Tsuruta and G. Nagayama, "Molecular dynamics studies on the condensation coefficient of water," J. Phys. Chem. B 108: 1736-1743 (2004).

[10] T. Ishiyama, T. Yano, and S. Fujikawa, "Molecular dynamics study of kinetic boundary conditions at an interface between argon vapor and its condensed phase," Phys. Fluids 16: 2899-2906 (2004).

[11] T. Ishiyama, T. Yano, and S. Fujikawa, "Molecular dynamics study of kinetic boundary conditions at an interface between a polyatomic vapor and its condensed phase," Phys. Fluids 16: 4713-4726 (2004).

[12] B.-Y. Cao, J.-F. Xie, and S.S. Sazhin, "Molecular dynamics study on evaporation and condensation of n-dodecane at liquid-vapour phase equilibria," J. Chem. Phys. 134: 164309 (2011).

[13] J.-F. Xie, S.S. Sazhin, and B.-Y. Cao, "Molecular dynamics study of the processes in the vicinity of the n-dodecane vapour/liquid interface," Phys. Fluids 23: 112104 (2011).

[14] B. Smit, S. Karaborni, and J.I. Siepmann, "Computer simulations of vapour-liquid phase equilibria of n-alkanes," J. Chem. Phys. 102: 2126-2140 (1995).

[15] M.P. Allen and D.J. Tildesley, *Computer Simulation of Liquids* (Clarendon, Oxford, 1987).

[16] P. van der Ploeg and H.J.C. Berendsen, "Molecular dynamics simulation of a bilayer membrane," J. Chem. Phys. 76: 3271-3276 (1982).

[17] W. L. Jorgensen, J. D. Madura, and C. J. Swenson, "Optimized intermolecular potential functions for liquid hydrocarbons," J. Am. Chem. Soc. 106: 6638-6646 (1984).

[18] J.B. Maxwell, *Data Book on Hydrocarbons: Application to Process Engineering* (Van Nostrand, Princeton, NJ, 1955).

[19] S. Fujikawa and M. Maerefat, "A study of the molecular mechanism of vapor condensation," JSME Int. J. Series II 33: 634-641 (1990).